NANO MICRO small

Supporting Information

for *Small*, DOI: 10.1002/smll.201805493

Rational Design of a Flexible CNTs@PDMS Film Patterned by Bio-Inspired Templates as a Strain Sensor and Supercapacitor

Chenjun Zhang, Hui Li, Aoming Huang, Qiao Zhang, Kun Rui, Huijuan Lin, Gengzhi Sun, Jixin Zhu,* Huisheng Peng, and Wei Huang*

Supporting Information

Rational Design of a Flexible CNTs@PDMS Film Patterned by Bio-Inspired Templates as a Strain Sensor and Supercapacitor

Chenjun Zhang, Hui Li, Aoming Huang, Qiao Zhang, Kun Rui, Huijuan Lin, Gengzhi Sun, Jixin Zhu,* Huisheng Peng, and Wei Huang*

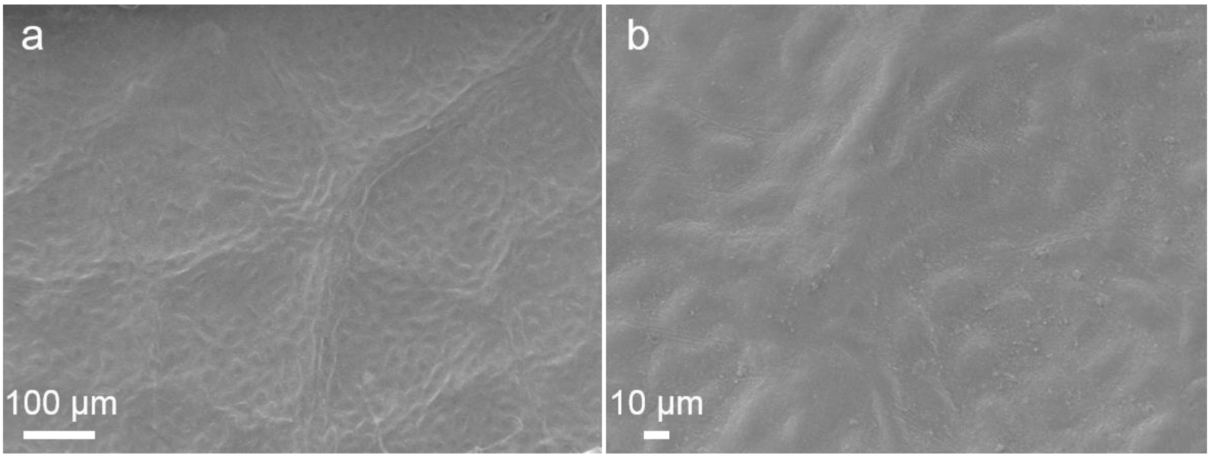

Figure S1. SEM images of the leaf surface at low (a) and high (b) magnifications, respectively.

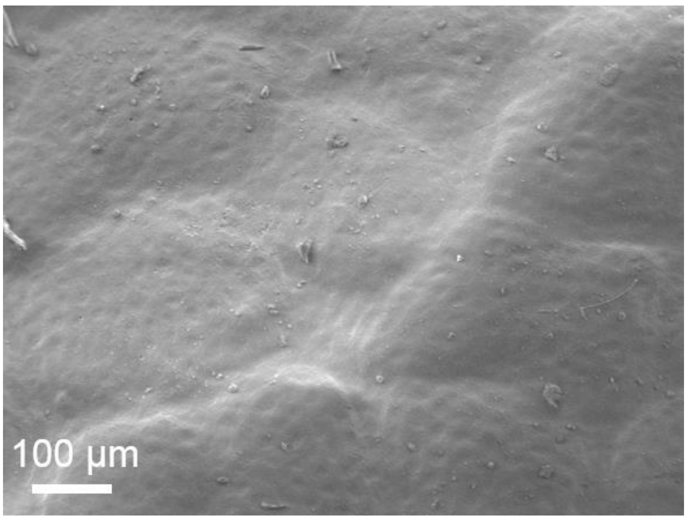

Figure S2. A SEM image of the P-PDMS film patterned by leaf template.

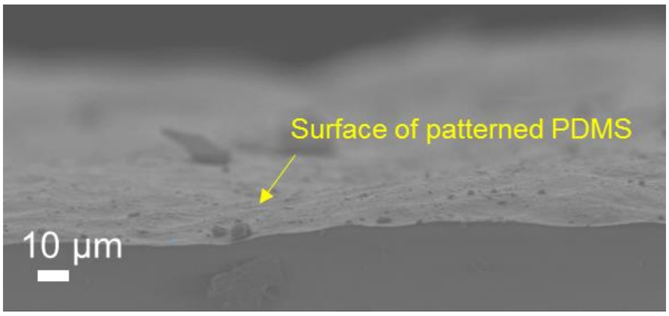

Figure S3. A cross-sectional SEM image of P-PDMS film.

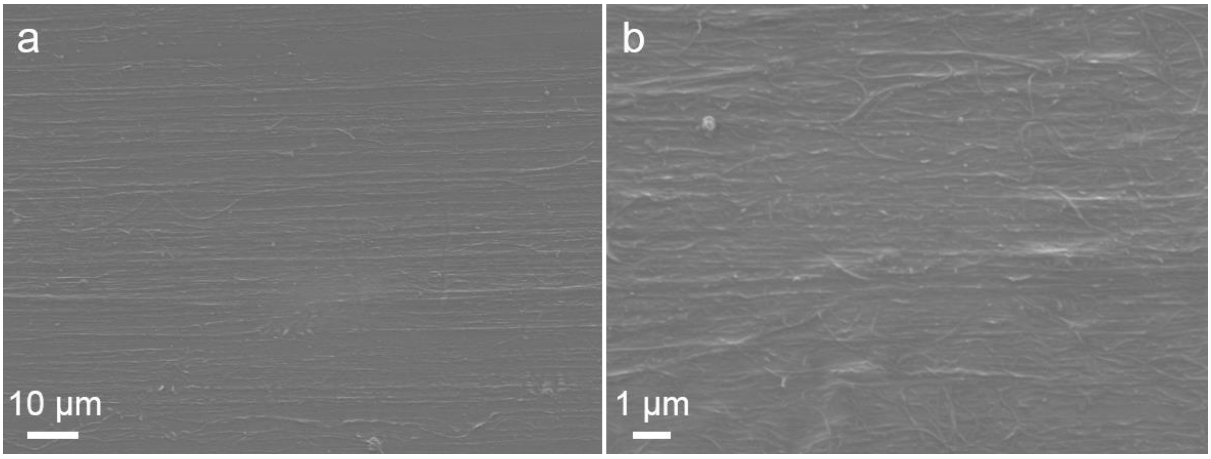

Figure S4. SEM images of CNT sheets paved on the P-PDMS film without pre-stretching process at low (a) and high (b) magnifications, respectively.

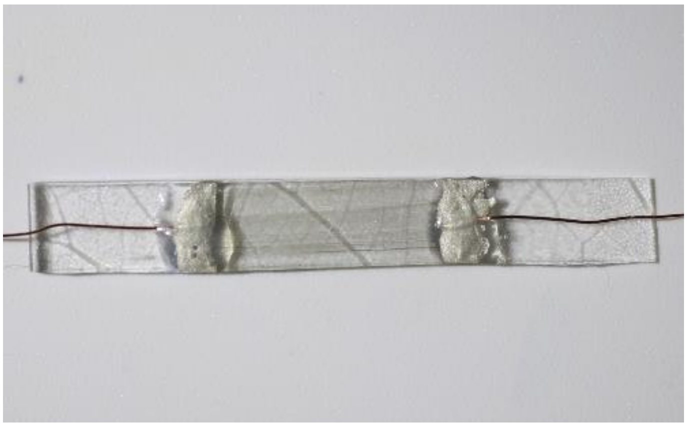

Figure S5. Photograph of the assembled CNTs@P-PDMS strain sensor.

Table S1. Comparison of the sensing performance of wrinkled CNTs@P-PDMS with the previous literature results.

Materials	Gauge factor	Strain range	Resistance response	Ref.
Wrinkled CNTs@P-PDMS	**0.4 (0-20%)** **5.5 (20-35%)** **22.6 (35-44%)**	**0-44%**	**3.0**	**This work**
Carbon nanofiber-PDMS	-	0-30%	0.6	[1]
CNT-PDMS	4.3	0-30%	1.1	[2]
CNT-PDMS	-	0-30%	2.1	[3]
Carbon paper-PDMS	25.3 (0-3%) 4.73 (3-15%)	0-20%	1.5	[4]
Silver nanowires-PDMS	2-14	0-60%	2.7	[5]
Graphene porous network-PDMS	2.6 (0-18%) 8.5 (22-40%)	0-40%	2.6	[6]
Silver nanoparticles-PDMS	2.05	0-20%	1.4	[7]
Graphene ripples-PDMS	2	0-20%	0.4	[8]
Carbon black particles-PDMS	5.5 (0-10%) 1.8 (>10%)	0-80%	1.5	[9]
Carbon thread-PDMS	8.7 (0-4%) 18.5 (8-10%)	0-10%	1.2	[10]

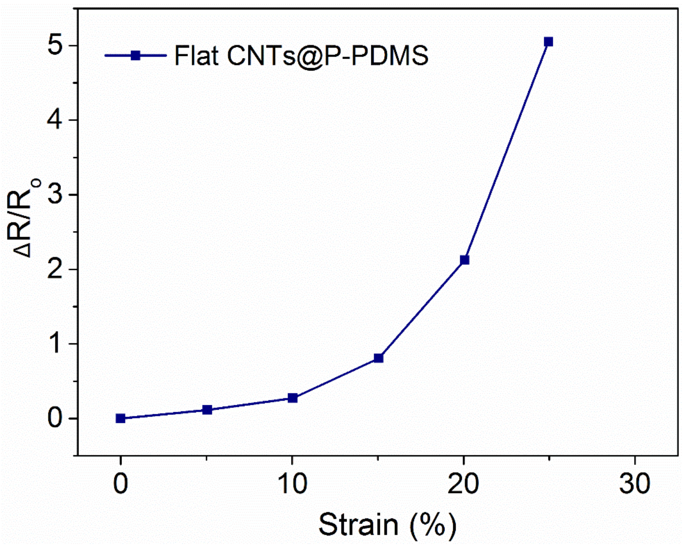

Figure S6. The plot of relative resistance of the flat CNTs@P-PDMS film without pre-stretching process as a function of tensile strain.

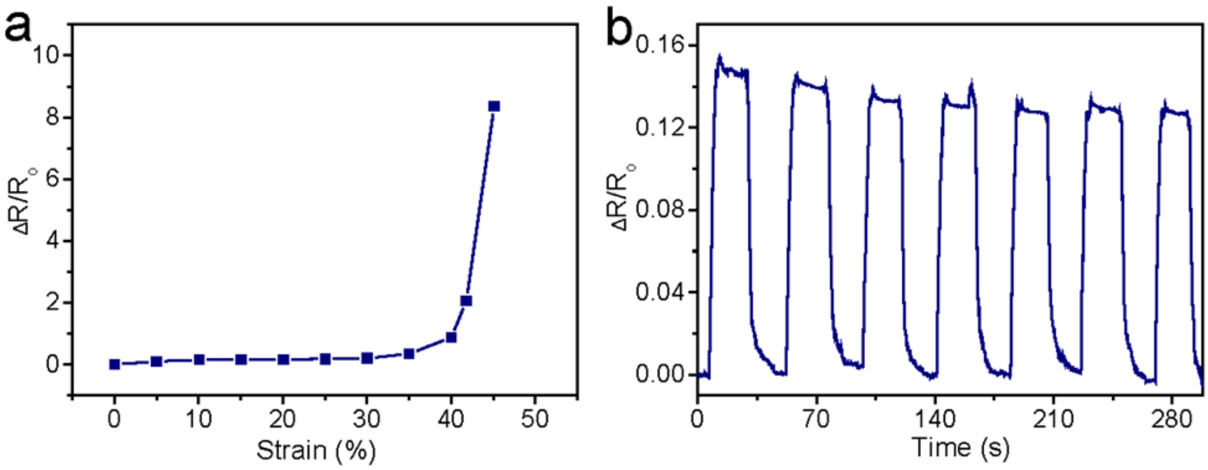

Figure S7. Sensing behavior of the wrinkled CNTs@P-PDMS film with 50% pre-strain. (a) The plot of relative resistance change of sensor as a function of tensile strain. (b) The relative resistance change under the cyclic strain between 0 to 20%.

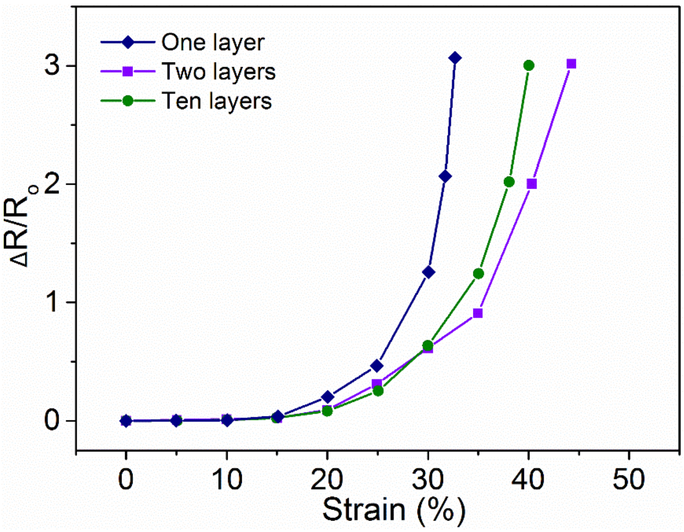

Figure S8. The plot of relative resistance of CNTs@P-PDMS films with different layers of CNTs sheets as a function of tensile strain.

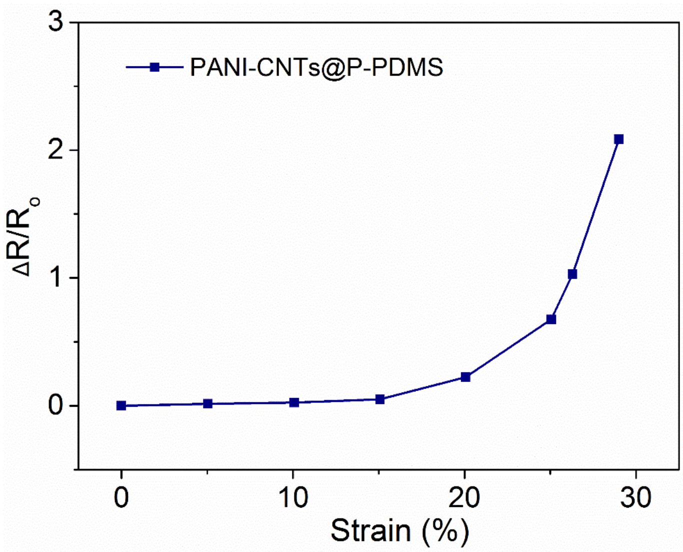

Figure S9. The plot of relative resistance of PANI-CNTs@P-PDMS as a function of tensile strain.

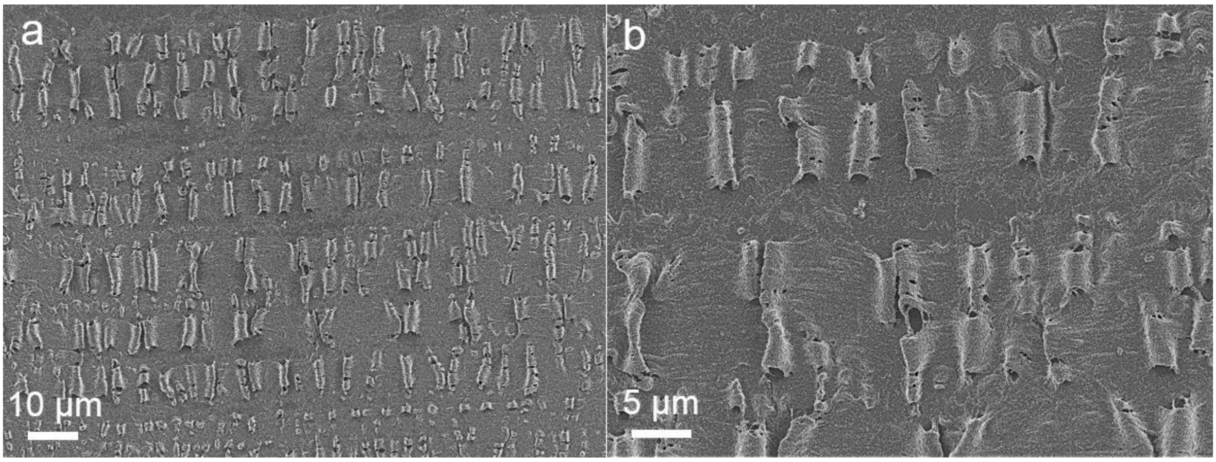

Figure S10. SEM images of PANI-CNTs@P-PDMS film with PANI weight percentage of 50% at low (a) and high (b) magnifications, respectively.

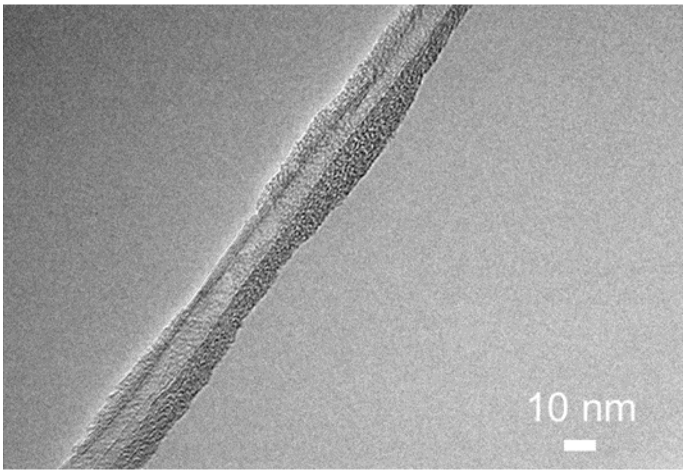

Figure S11. A typical TEM image of CNTs sheets with 50% PANI.

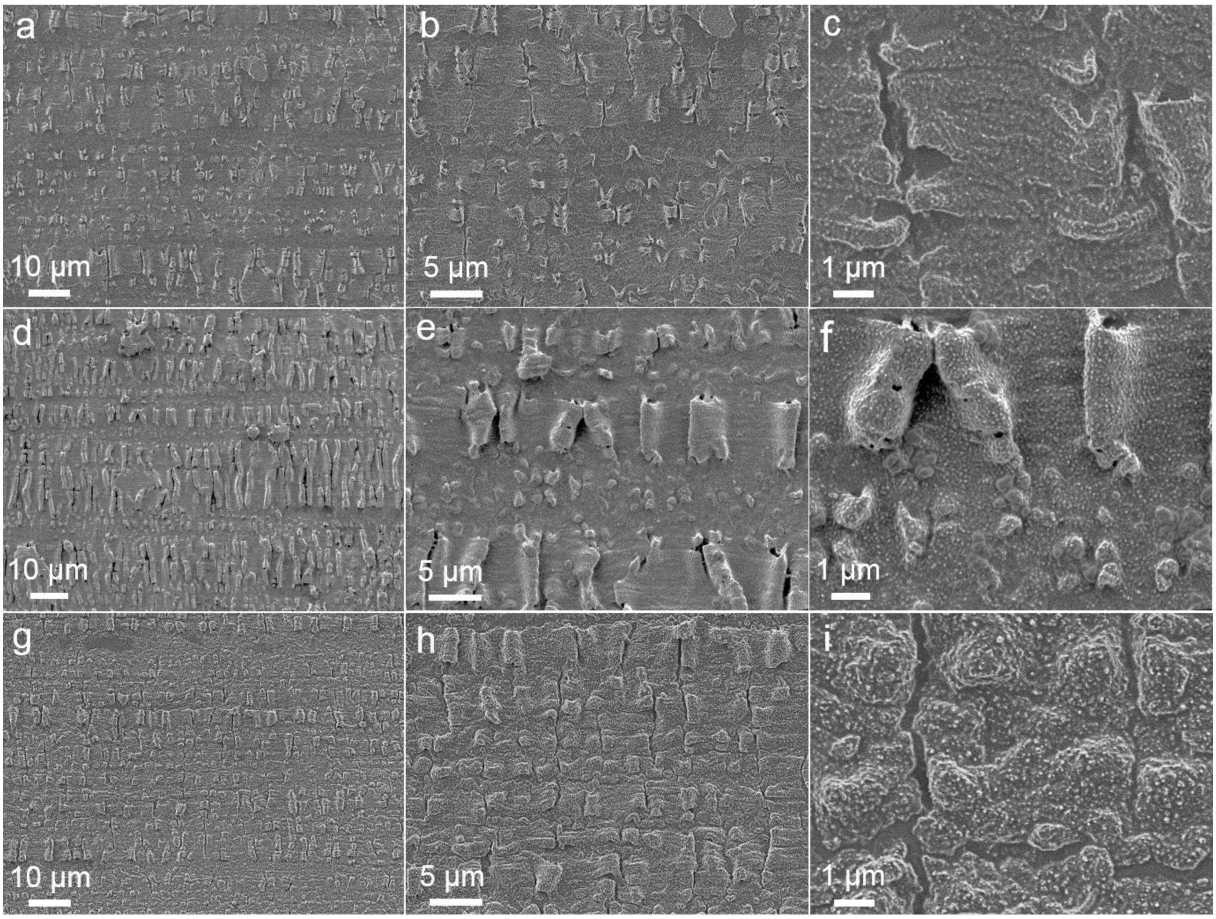

Figure S12. SEM images of PANI-CNTs@P-PDMS film with PANI weight percentage of 20% (a-c), 70% (d-f), 85% (g-i) in different magnifications.

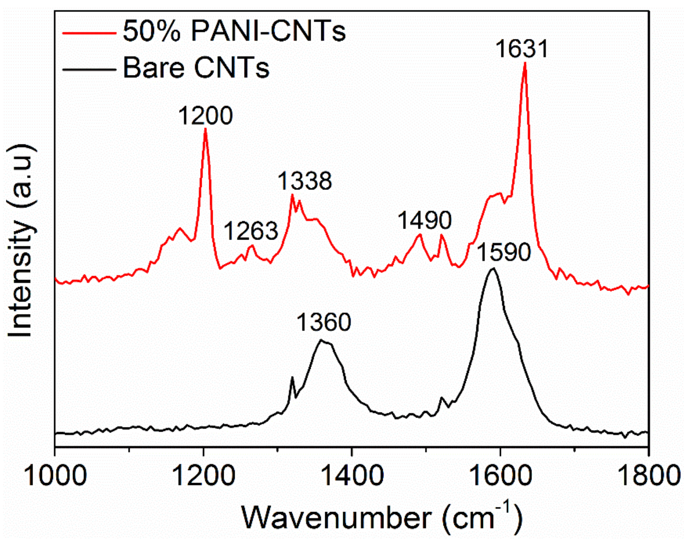

Figure S13. Raman spectra of bare CNTs and PANI-CNTs film with PANI weight percentage of 50%.

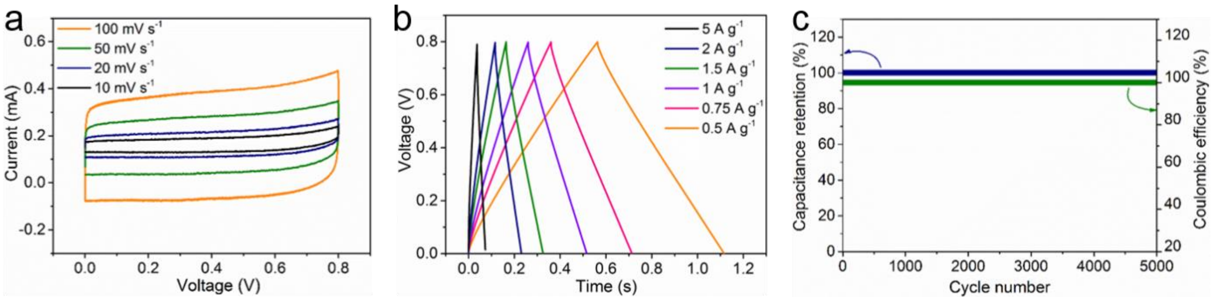

Figure S14. Electrochemical performance of the supercapacitor based on bare CNTs. (a) CV curves at a scan rate from 10 mV s^{-1} to 100 mV s^{-1}. (b) Charge-discharge curves at a current density from 0.5 A g^{-1} to 5 A g^{-1}. (c) Cycling measurement at 1 A g^{-1}.

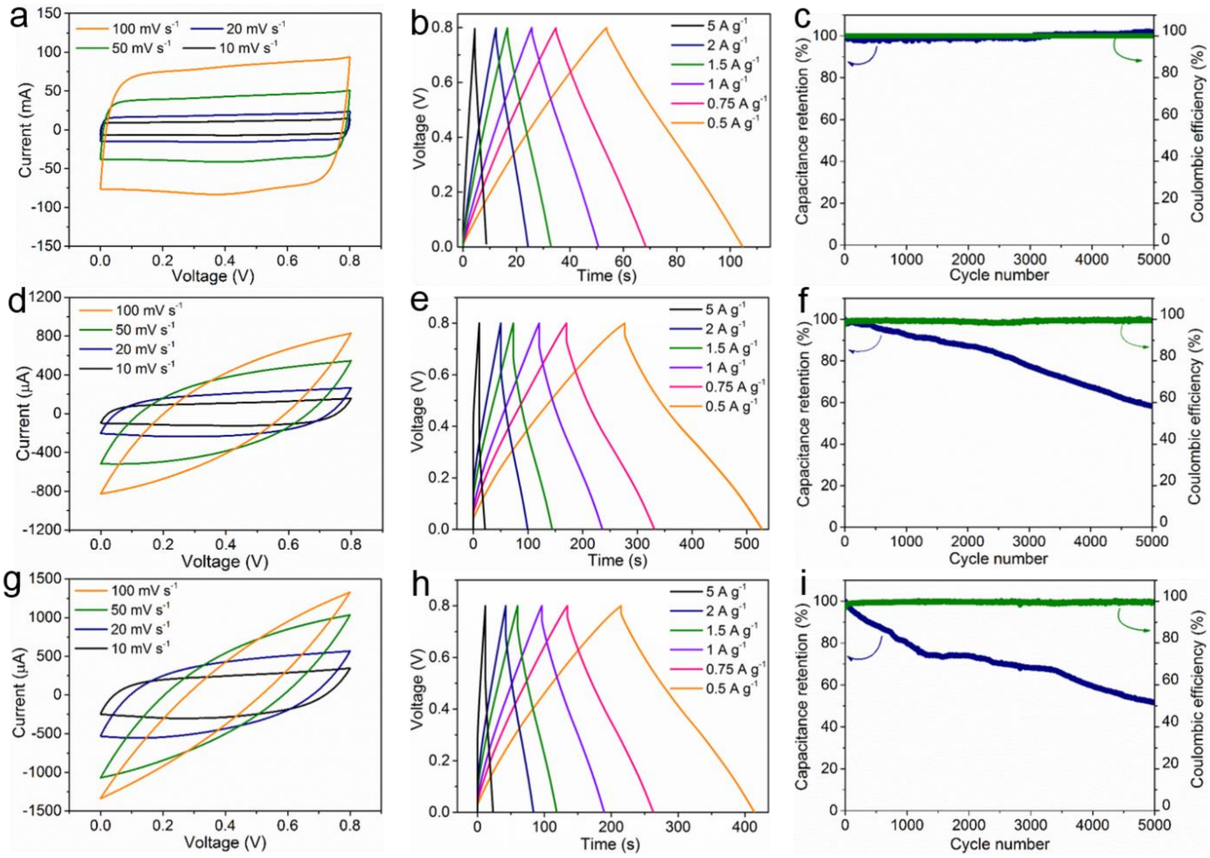

Figure S15. Electrochemical performance of supercapacitors based on PANI-CNTs with PANI weight percentage of 20% (a-c), 70% (d-f), 85% (g-i). (a, d, g) CV curves at a scan rate of 10 mV s^{-1} to 100 mV s^{-1}. (b, e, h) Charge-discharge curves at a current density from 0.5 A g^{-1} to 5 A g^{-1}. (c, f, i) Cycling measurements at 1 A g^{-1}.

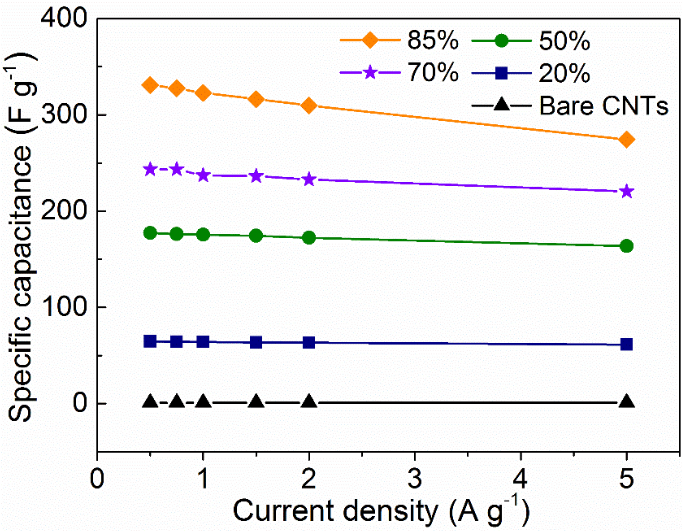

Figure S16. Electrochemical rate performance of the supercapacitors based on bare CNTs and PANI-CNTs with PANI weight percentage of 20%, 50%, 70% and 85%. The specific capacitance was calculated according to the charge-discharge curves at the current densities of 0.5, 0.75, 1, 1.5, 2, 5 A g^{-1}.

Table S2. Comparison of the electrochemical performance of wrinkled 50% PANI-CNTs@P-PDMS with the previous literature results.

Materials	Specific capacitance ($F\ g^{-1}$)	Cycle number	Capacitance retention	Ref.
Wrinkled 50% PANI-CNTs@P-PDMS	**176 at 1 A g^{-1}**	**10000**	**88%**	**This work**
Graphene-PANI	60 at 1.26 A g^{-1}	17000	86%	[11]
CNTs-PANI (50%)	233 at 1 A g^{-1}	1000	>100%	[12]
CNTs-PANI (50%)	200 at 1 A g^{-1}	2000	~100%	[13]
Graphene oxide-PANI (50%)	130 at 1 A g^{-1}	5	100%	[14]
MnO_2-PANI	129 at 0.5 A g^{-1}	5000	84.7%	[15]
Pt-CNT-PANI	86.2 F g^{-1} at 0.5 mV s^{-1}	-	-	[16]
Nano graphene plates-PANI (50%)	~80 F g^{-1} at 1 A g^{-1}	1000	>100%	[17]
Graphene-PANI	198 F g^{-1} at 3 A g^{-1}	800	78%	[18]

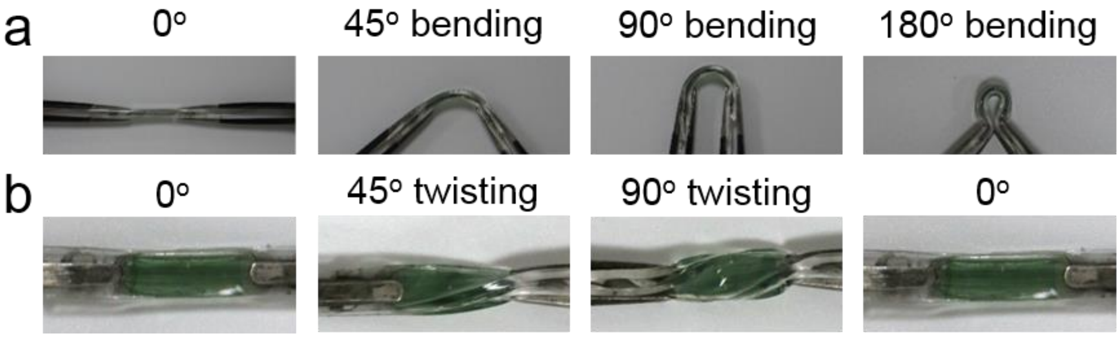

Figure S17. Mechanical flexibility of PANI-CNTs@P-PDMS supercapacitor. Photographs of a supercapacitor under (a) bending and (b) twisting in different angles.

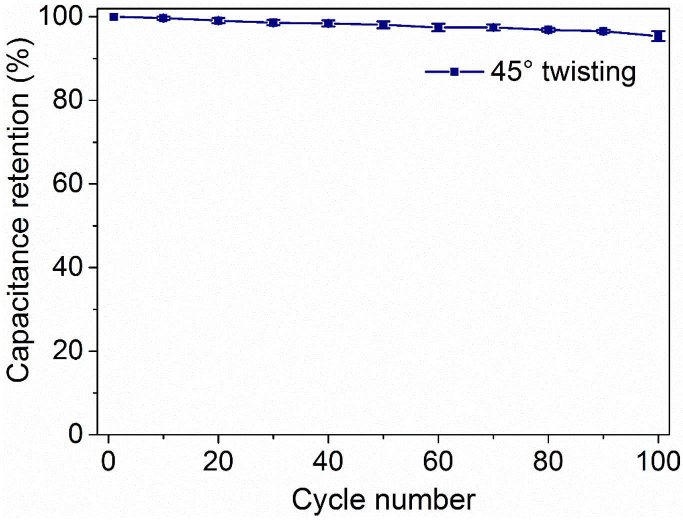

Figure S18. Dependence of capacitance retention on cycle number under 45° twisting.

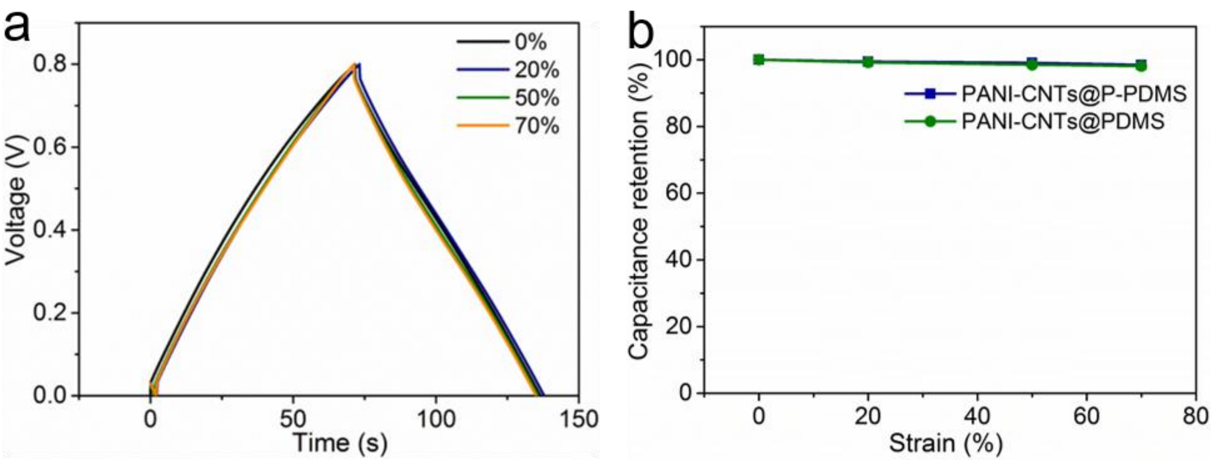

Figure S19. (a) The charge-discharge curves of the PANI-CNTs@P-PDMS supercapacitor with the strain ranging from 0 to 70%. (b) Capacitance retention of the PANI-CNTs@PDMS and PANI-CNTs@P-PDMS supercapacitors at corresponding strain.

Supplementary references

[1] S. A. Chowdhury, M. C. Saha, S. Patterson, T. Robison, Y. Liu, *Adv. Mater. Technol.* **2019**, *4*, 1800398.
[2] M. Abshirini, M. Charara, Y. Liu, M. Saha, M. C. Altan, *Adv. Eng. Mater.* **2018**, *20*, 1800425.
[3] J. Lee, M. Lim, J. Yoon, M. S. Kim, B. Choi, D. M. Kim, D. H. Kim, I. Park, S. J. Choi, *ACS Appl. Mater. Interfaces* **2017**, *9*, 26279.
[4] Y. Li, Y. A. Samad, T. Taha, G. Cai, S.-Y. Fu, K. Liao, *ACS Sustain. Chem. Eng.* **2016**, *4*, 4288.
[5] M. Amjadi, A. Pichitpajongkit, S. Lee, S. Ryu, I. Park, *ACS Nano* **2014**, *8*, 5154.
[6] Y. Pang, H. Tian, L. Tao, Y. Li, X. Wang, N. Deng, Y. Yang, T. L. Ren, *ACS Appl. Mater. Interfaces* **2016**, *8*, 26458.
[7] J. Lee, S. Kim, J. Lee, D. Yang, B. C. Park, S. Ryu, I. Park, *Nanoscale* **2014**, *6*, 11932.
[8] Y. Wang, R. Yang, Z. Shi, L. Zhang, D. Shi, E. Wang, G. Zhang, *ACS Nano* **2011**, *5*, 3645.
[9] J.-H. Kong, N.-S. Jang, S.-H. Kim, J.-M. Kim, *Carbon* **2014**, *77*, 199.
[10] Y. Q. Li, P. Huang, W. B. Zhu, S. Y. Fu, N. Hu, K. Liao, *Sci Rep* **2017**, *7*, 45013.
[11] P. Li, Z. Jin, L. Peng, F. Zhao, D. Xiao, Y. Jin, G. Yu, *Adv. Mater.* **2018**, *30*, 1800124.
[12] H. Lin, L. Li, J. Ren, Z. Cai, L. Qiu, Z. Yang, H. Peng, *Sci. Rep*. **2013**, *3*, 1353.
[13] X. Chen, H. Lin, P. Chen, G. Guan, J. Deng, H. Peng, *Adv. Mater.* **2014**, *26*, 4444.
[14] K. Zhang, L. L. Zhang, X. S. Zhao, J. Wu, *Chem. Mater.* **2010**, *22*, 1392.
[15] K. Ghosh, C. Y. Yue, M. M. Sk, R. K. Jena, *ACS Appl. Mater. Interfaces* **2017**, *9*, 15350.
[16] D. Zhang, M. Miao, H. Niu, Z. Wei, *ACS Nano* **2014**, *8*, 4571.
[17] Y. Xu, M. G. Schwab, A. J. Strudwick, I. Hennig, X. Feng, Z. Wu, K. Müllen, *Adv. Energy Mater*. **2013**, *3*, 1035.
[18] Q. Wu, Y. Xu, Z. Yao, A. Liu, G. Shi, *ACS Nano* **2010**, *4*, 1963.